Davis and G. J. Walker, Univ. of Tasmania, Australia, 1992, pp. 219–222.

[3]Standingford, D. W. F., Lazauskas, L. V., and Tuck, E. O., "On the Numerics of the Lifting Surface Equation," Applied Mathematics Dept., Univ. of Adelaide, Adelaide, Australia, 1995.

[4]Tuck, E. O., "Some Accurate Solutions of the Lifting Surface Equation," *Journal of the Australian Mathematical Society (Series B)*, Vol. 35(2), Oct. 1993, pp. 127–144.

[5]Lan, C. E., "A Quasi-Vortex-Lattice Method in Thin Wing Theory," *Journal of Aircraft*, Vol. 11, No. 9, 1974, pp. 518–527.

[6]Turrill, D., "Wings and Free Speed," *Open Wheel Magazine*, May 1992, p. 63.

Multiple Design Point Optimization of High-Speed Proprotors

Aditi Chattopadhyay,* Thomas R. McCarthy,† and Charles E. Seeley†
Arizona State University, Tempe, Arizona 85287-6106

Introduction

RECENTLY, Chattopadhyay et al.[1] developed a multilevel decomposition-based optimization procedure for improved high-speed cruise and hovering performance of tiltrotor aircraft. The goal of that study was to improve aerodynamic performance in hover and cruise in the upper level and to improve structural characteristics in these flight modes at the lower level. The aerodynamic analysis used in Ref. 1 was based on blade element approach and two-dimensional airfoil theories. These were later corroborated by Dadone et al.[2] in a parametric study conducted to investigate the important design issues associated with the development of high-speed proprotors using a comprehensive Euler analysis.

This study extends the work of Ref. 1 by including takeoff performance in the optimization formulation. The aerodynamic and structural design criteria in high-speed cruise, hover, and takeoff are addressed using a multilevel decomposition-based optimization procedure. At the upper level, the aerodynamic performance of proprotors is optimized for each flight condition using planform variables. Constraints are imposed on the rotor thrust in all three flight conditions. A nonlinear programming technique based on the Broyden–Fletcher–Goldfarb–Shanno (BFGS) algorithm is used for the optimization. At the lower level, the rotor is optimized for improved structural performance using composite ply-stacking sequence as a design variable. Since only discrete design variables are used at the lower level, an optimization procedure based on simulated annealing algorithm[3] is developed to address this complex problem. Only the major findings of this study are presented in this note and the interested reader should consult Refs. 1 and 4 for complete details of the problem formulation.

Optimization Problem

The following is a brief description of the two-level optimization problem. Detailed explanations are found in Refs. 1 and 4.

Received Dec. 29, 1995; revision received Jan. 24, 1996; accepted for publication Feb. 12, 1996.

*Associate Professor, Department of Mechanical and Aerospace Engineering, Associate Fellow AIAA.

†Graduate Research Associate, Department of Mechanical and Aerospace Engineering. Student Member AIAA.

Upper Level

The axial efficiency in high-speed cruise η_c and the figure of merit in both hover and in takeoff (FM_h and FM_t, respectively) are maximized simultaneously in this level using aerodynamic design variables. Constraints are imposed on the rotor thrust at each of these flight conditions. Geometric constraints are also imposed on the physical dimensions of the blade to ensure that the load-carrying member of the rotor is maintained within the dimensions of the airfoil. The blade is discretized and design variables include the values of chord c, twist θ, thickness-to-chord ratio t/c, and zero-lift angle of attack α_{zl} at each node. A quadratic variation with no initial offset is used to represent the lifting line to ensure continuity of the elastic axis. The parameter that determines the quadratic variation is also used as a design variable.

Lower Level

The structural characteristics of the rotor are investigated at this level. The objectives are to minimize the tip displacements in cruise, hover, and takeoff. The most critical of these displacements are included in the formulation. In cruise, the elastic twist ϕ_c and the in-plane displacement v_c are critical. In hover and in takeoff conditions, the vertical displacement (w_h and w_t, respectively), and the elastic twist (ϕ_h and ϕ_t, respectively), are significant. Therefore, these six displacements are selected as the individual objective functions to be minimized. Ply orientations are used as design variables. However, to avoid impractical values the ply angles are chosen from a set of preselected values (0, ±15, ±30, . . . , 90 deg). Stress constraints are imposed based on the Tsai-Wu failure criterion[5] on each lamina at each of the four corners of the box beam to prevent failure because of stresses.

Results

The reference rotor used is an existing advanced three-bladed gimballed rotor.[6] The aerodynamic optimization in high-speed cruise is performed at a cruise altitude of 25,000 ft and a forward velocity of 300 kn with a rotational speed of 421 rpm. A vehicle weight of 13,000 lb and aircraft lift-to-drag ratio L/D of 8.4 is assumed. Therefore, the thrust in cruise is constrained to be 774 lb for the two-engine aircraft. In hover, the aircraft is assumed to be operating at sea level conditions with a rotational speed of 570 rpm and a 12% download effect from the rotor/wing interaction. The thrust in hover is therefore constrained to be at 7280 lb. To simulate the takeoff condition a load factor of 1.25 is used. Inclusion of the 12% download effect results in a takeoff thrust of 9100 lb. A rotational speed of 570 rpm is used and an altitude of 6695 ft is assumed to simulate a high-altitude takeoff. A composite rotor blade made of Carbon-PEEK AS4/APC2 (Ref. 7) is used. The blade is discretized into 10 segments.

The nodal values of c, θ, α_{zl}, and t/c are used as design variables at the upper level. The sweep distribution Λ is based on a quadratic lifting line. This yields a total of 45 design variables. An in-house code based on the Kreisselmeier–Steinhauser (K–S) function, developed at Arizona State University,[4] is used as the optimization algorithm at this level. The search direction used during optimization is based on the BFGS algorithm[8] and the two-point exponential expansion is used to approximate the objective functions and constraints.

At the lower level, the design variables used represent discrete values of the composite ply orientations. A symmetric and balanced lay-up is assumed in both the vertical and the horizontal walls. This leads to 12 independent design variables that can assume any one of the seven preselected values of ply-angle orientations. The results from this multiple design point optimization are presented in Table 1 and Figs. 1a–1d.

The upper level objective functions are presented in Table 1. The figures of merit in hover FM_h and in takeoff FM_t are increased by 6.9 and 31%, respectively, from the reference values. A small increase (0.52%) is obtained in the cruise pro-

Table 1 Summary of optimum results

Objective functions[a]	Reference value	Optimum value	Percentage change
Level 1			
FM_h	0.760	0.813	+6.9
η_c	0.888	0.893	+0.52
FM_t	0.617	0.807	+31.0
Level 2			
Flap, w_h, in.	11.5	6.95	−40.0
Lag, v_c, in.	−2.21	−1.03	−42.0
Flap, w_t, in.	13.7	7.91	−54.0
Twist, ϕ_h, deg	−2.05	−1.77	−14.0
Twist, ϕ_c, deg	−1.22	−1.19	−42.0
Twist, ϕ_t, deg	−1.73	−1.39	−20.0

[a]Subscripts h, c, and t denote hover, cruise and takeoff conditions, respectively.

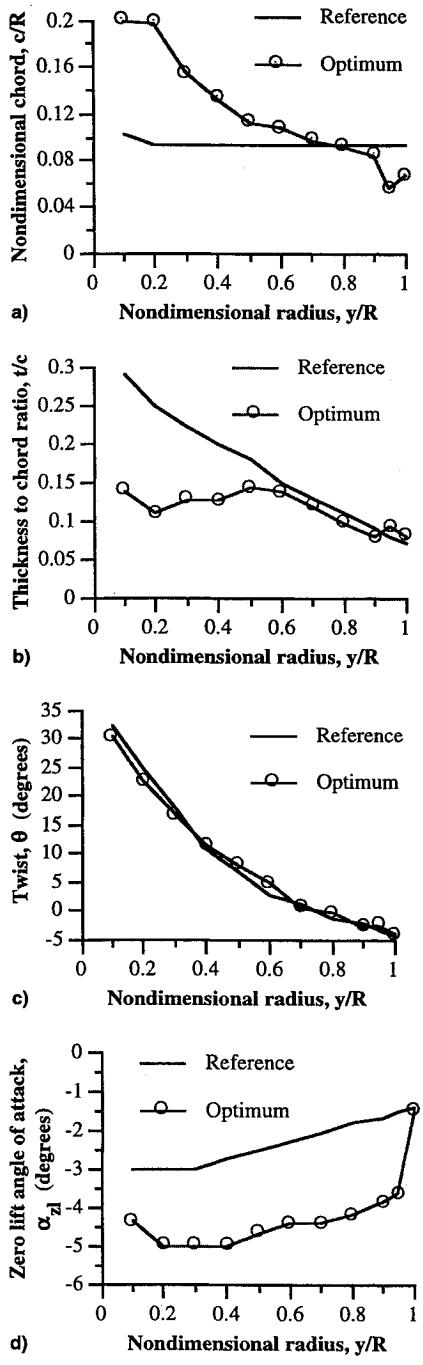

Fig. 1 Comparison of optimum and reference rotor distributions: a) chord, b) thickness-to-chord ratio, c) blade twist, and d) zero-lift angle of attack.

pulsive efficiency η_c as well. These trends can be explained by examining the rotor planform.

A comparison of the optimum and reference chord distributions c are shown in Fig. 1a and significant differences must be noted. The optimum distribution closely resembles the well-known ideal hover planform with notable exceptions at the root and at the tip. The proximity to the hover planform is because of the large solidity necessary to achieve the thrust required in both hover and takeoff. The deviation (from ideal hover planform) at the root is a result of an upper bound of 0.2, which is imposed on the nondimensional chord c/R to avoid large chord sections. The deviation at the tip is because of a geometric constraint imposed to ensure that the box beam is maintained within the airfoil section. The reduction in the outboard section, relative to the reference rotor, is attributable to the lack of any maneuver margin requirement in the optimization problem formulation.

The t/c distributions of the reference and the optimum rotor configurations are presented in Fig. 1b and show large reductions from the reference rotor at the inboard sections of the optimum rotor. The thickness is also slightly reduced from the reference values at midspan locations and is slightly increased at the tip. The former is explained as an attempt to improve the rotor performance by reducing the profile drag. The latter represents the optimizer's effort to satisfy the geometric constraint that ensures that the box beam is contained within the airfoil section. Since the optimum distribution is very similar to the reference distribution at midspan locations and slight increases are observed at the tip, the profile drag over the working section of the blade in case of high-speed cruise is only slightly altered. This, coupled with the chord distribution over this section of the blade, results in only a slight improvement of the high-speed cruise propulsive efficiency η_c.

The twist distributions θ, presented in Fig. 1c, are reduced from reference to optimum values over the inboard section of the blade, increased over the midspan section, and show virtually no change in the outboard section. The increase is achieved in a region of the blade that has greater resultant velocities. This lowers the collective pitch, thereby reducing the overall angle of the attack of the blade. The result is a more even distribution of the angle of attack throughout the blade, which subsequently reduces drag. In case of high-speed cruise, the inflow angle is only slightly changed between reference and optimum, which partially explains the very small improvements obtained in η_c.

The zero-lift angle-of-attack distributions α_{zl} (Fig. 1d) show significant decreases after optimization, except at the tip. The result is an increase in airfoil camber that improves the lift-to-drag ratio, thereby improving performance. The increased camber, however, leads to higher drag divergence Mach numbers M_{dd}, which can adversely affect cruise performance. Therefore, to avoid large drag penalties caused by operating the blade at local Mach numbers above M_{dd}, the zero-lift angle of attack is only slightly reduced at the tip.

Since only static loading is included in this study and no aeroelastic stability requirements are imposed during optimization, the rotor was only allowed to have backward sweep. However, backward sweep induces large nose-down pitching moments. This increases the magnitude of the elastic twist, which represents an objective function to be minimized at each flight condition. As a result, the optimizer avoids sweeping the blades to remain in the feasible domain.

The lower level objective functions are presented in Table 1 where large reductions from the reference rotor are observed in all six objective functions. The composite laminate stacking sequences are also presented in Table 2. Note that in the reference blade, the horizontal and vertical walls are assumed to have the same stacking sequence. Further, since all of the laminates are considered to be symmetric, only 12 of the 24 total plies are presented. The individual ply thickness used in this study is 0.001 in. The rearrangement of the stacking sequence

Table 2 Summary of optimum results, stacking sequence of symmetric 24-ply laminated walls

Stacking sequence	Reference horizontal and vertical wall, deg	Optimum horizontal wall, deg	Optimum vertical wall, deg
θ_1	Outer ply, 0	15	15
θ_2	0	−15	−15
θ_3	0	0	−15
θ_4	0	0	−15
θ_5	15	45	30
θ_6	−15	−45	−30
θ_7	15	45	30
θ_8	−15	−45	−30
θ_9	45	0	0
θ_{10}	−45	0	0
θ_{11}	45	30	15
θ_{12}	Midplane, −45	−30	−15

after optimization represents a compromise between the conflicting requirements of reduced elastic twist and reduced transverse displacements. This is observed by noting the inclusion of ±30-deg plies in both the horizontal and the vertical walls. The reductions in all of the tip displacements are attributable to the improved ply-stacking sequence and the increased thickness of the airfoil caused by larger chords, which in turn increases the box beam height.

Concluding Remarks

The results of a multiple design point optimization procedure for design of high-speed proprotors were presented. The procedure was based on multilevel decomposition and a multiobjective formulation that used the K–S function technique. Aerodynamic performance was the objective of the upper level and the structural response was improved at the lower level. Optimization was performed simultaneously to include design criteria from high-speed cruise, hover, and takeoff. A nonlinear programming technique was used at the upper level and a simulated annealing algorithm was used for the discrete optimization problem at the lower level. The optimum results were compared with a reference rotor. The following are some important observations:

1) The multilevel optimization procedure significantly improves the aerodynamic and structural response of the high-speed proprotor blade at all three flight conditions.

2) Optimum planform distributions represent compromises between the conflicting requirements of the three flight conditions. At locations near the root and the tip, the optimizer is driven by the geometric constraints imposed on the problem.

3) The simulated annealing algorithm successfully minimizes the tip displacements by altering the composite plate stacking sequences in the horizontal and vertical walls. The optimum stacking sequence represents a compromise between reduced elastic twist and reduced transverse deformation. This is manifested through the selection of ±30-deg plies in both the horizontal and the vertical walls.

4) A combination of improved stacking sequence and larger chord values leads to reduced elastic deformation in the optimum configurations.

Acknowledgment

The authors acknowledge the support of this research through a grant from NASA Ames Research Center, Grant NCC2-795, Technical Monitors were John F. Madden III and Sesi Kottapalli.

References

[1]Chattopadhyay, A., McCarthy, T. R., and Seeley, C. E., "A Decomposition Based Optimization Procedure for High Speed Prop-Rotors Using Composite Tailoring and Simulated Annealing," *Journal of Aircraft*, Vol. 32, No. 5, 1995, pp. 1026–1033.

[2]Dadone, L., Liu, J., Wilkerson J., and Acree, C. W., "Proprotor Design Issues for High Speed Tiltrotors," *Proceedings of the 50th Annual Forum of the American Helicopter Society*, American Helicopter Society, Washington, DC, 1994.

[3]Chattopadhyay, A., and Seeley, C. E., "A Simulated Annealing Technique for Multiobjective Optimization of Intelligent Structures," *Journal of Smart Materials and Structures*, Vol. 3, June 1994, pp. 98–106.

[4]Chattopadhyay, A., McCarthy, T. R., and Seeley, C. E., "A Multiple Design Point Optimization of High Speed Proprotors," *Proceedings of the 20th European Rotorcraft Forum* (Amsterdam, The Netherlands), 1994 (Paper 47).

[5]Tsai, S. W., and Wu, E. M., "A General Theory of Strength for Anisotropic Materials," *Journal of Composite Materials*, Vol. 5, Jan. 1971, pp. 58–80.

[6]Lamon, S., "XV-15 Advanced Technology Blades, Ultimate Stress Analysis," Boeing Rept. D210-12345-1, 1985.

[7]Agarwal, B. D., and Broutman, L. J., *Analysis and Performance of Fiber Composites*, Wiley, New York, 1990.

[8]Haftka, R. T., Gürdal, Z., and Kamat, M. P., *Elements of Structural Optimization*, Kluwer, Dordrecht, The Netherlands, 1990.

Identification of Lateral–Directional Behavior in Stall from Flight Data

J. Singh* and R. V. Jategaonkar†
DLR, German Aerospace Research Establishment, D-38108 Brunswick, Germany

Introduction

AERODYNAMICS associated with aircraft flight in stall and poststall regimes are of increasing interest. Computational fluid dynamic methods[1,2] and a number of semiempirical models[3,4] have resulted in a significantly improved modeling of unsteady stalled flow. Much of the research work is, however, based on wind-tunnel data from unsteady airfoil tests and only a few applications to identification from flight data have been reported.[5,6] Moreover, analysis in the stall and poststall region is more or less confined only to the longitudinal dynamics. Recently, based on a state–space representation of unsteady aerodynamics at high angle of attack,[7] the problem of stall identification from flight data pertaining to the longitudinal dynamics has been addressed.[8] Flight analysts have, however, encountered cases in the past where an aircraft in stall is known to have exhibited large excursions in the lateral–directional motion. This behavior is attributed mainly to the significant sideforce and yawing moments generated because of formation and shedding of the forebody vortices.[9,10]

In this Note, the stall model is extended to asymmetric unsteady flow phenomenon and applied to identify, from flight data, the lateral–directional behavior of the C-160 aircraft. Both dynamic and quasisteady stall maneuvers are analyzed. It is observed that different flow separation points on the left and the right wing surfaces adequately characterize the pronounced variations in the lateral–directional motion of the quasisteady stall.

Stall Modeling

The trailing-edge stall is a dominating phenomenon on wings having sufficient thickness ($t/\bar{c} > 0.15$; where t repre-

Received July 7, 1995; revision received Nov. 8, 1995; accepted for publication Dec. 4, 1995.

*Guest Scientist, Institute of Flight Mechanics. Member AIAA.
†Senior Scientist, Institute of Flight Mechanics. Member AIAA.